AIP | Review of Scientific Instruments

Accurate spring constant calibration for very stiff atomic force microscopy cantilevers

Scott J. Grutzik, Richard S. Gates, Yvonne B. Gerbig, Douglas T. Smith, Robert F. Cook et al.

Citation: Rev. Sci. Instrum. **84**, 113706 (2013); doi: 10.1063/1.4832978
View online: http://dx.doi.org/10.1063/1.4832978
View Table of Contents: http://rsi.aip.org/resource/1/RSINAK/v84/i11
Published by the AIP Publishing LLC.

Accurate spring constant calibration for very stiff atomic force microscopy cantilevers

Scott J. Grutzik,[1] Richard S. Gates,[2] Yvonne B. Gerbig,[2] Douglas T. Smith,[2] Robert F. Cook,[2] and Alan T. Zehnder[1,a)]
[1]*Field of Theoretical and Applied Mechanics, Cornell University, Ithaca, New York 14853, USA*
[2]*Nanomechanical Properties Group, Material Measurement Laboratory, National Institute of Standards and Technology, Gaithersburg, Maryland 20899, USA*

(Received 10 July 2013; accepted 10 November 2013; published online 26 November 2013)

There are many atomic force microscopy (AFM) applications that rely on quantifying the force between the AFM cantilever tip and the sample. The AFM does not explicitly measure force, however, so in such cases knowledge of the cantilever stiffness is required. In most cases, the forces of interest are very small, thus compliant cantilevers are used. A number of methods have been developed that are well suited to measuring low stiffness values. However, in some cases a cantilever with much greater stiffness is required. Thus, a direct, traceable method for calibrating very stiff (approximately 200 N/m) cantilevers is presented here. The method uses an instrumented and calibrated nanoindenter to determine the stiffness of a reference cantilever. This reference cantilever is then used to measure the stiffness of a number of AFM test cantilevers. This method is shown to have much smaller uncertainty than previously proposed methods. An example application to fracture testing of nanoscale silicon beam specimens is included. © *2013 AIP Publishing LLC*. [http://dx.doi.org/10.1063/1.4832978]

I. INTRODUCTION

Atomic force microscopy (AFM), a variant of scanning probe microscopy, is a dominant instrument for mechanical properties measurements at the nano- and micro-scales. Measurements of mechanical properties, especially force-displacement responses, using AFM have been performed on systems ranging from the extremely compliant, such as molecular layers and cell membranes,[1,2] using very small forces (pN to nN), to the very stiff, such as silicon (Si) components of microelectromechanical systems (MEMS) devices,[3] using much larger forces (up to 100s of μN).

The central element of most AFM instruments is a cantilever that deforms in response to contact with, or proximity to, the surface of the material or system being measured. In particular, the deflection or change in orientation of the free end of the cantilever is detected using diode-based position sensitive detectors (PSDs) that record the motion of a laser spot reflected from the back of the cantilever as the deflection changes. As the length/thickness ratio of the cantilever is usually very large, the displacement of the free end of the cantilever, Δz, is linearly related to the deflection. The change in force, ΔP, exerted by the cantilever on the surface is related to the displacement, Δz, by the cantilever stiffness, $k = dP/dz$. Hence, once a relationship between PSD output voltage and Δz of an AFM is established, ΔP can be determined if k is known or calibrated.

Compliant cantilevers are used for mechanical properties measurements such as molecular adhesion, as the displacement, and hence deflection, of the cantilever is large enough to generate measurable spot motion on the PSD under the influence of the very small forces involved. There are many methods available for calibrating the stiffness of such cantilevers, which typically have k values in the range 0.01 N/m to 1 N/m.[4] Many of these methods are based on measuring vibrational or resonance characteristics of the cantilever and using these characteristics to determine cantilever stiffness through mechanical or thermodynamic relations.[5] The large vibrational amplitudes and small resonant frequencies of compliant cantilevers enable the instrumentation within most commercial AFMs to implement these methods, often in an automated manner, and they suffice for most AFM applications.[4]

Stiff cantilevers are required for mechanical properties measurements involving bulk material deformation, such as the fracture of nanoscale Si beams,[6,7] as the forces required are quite large by AFM standards. Because of high frequencies and small amplitudes, vibrational methods are poorly suited to calibrating the stiffness of such cantilevers, which, in the case of the nanoscale beam fracture measurements, had k values in the range 200 N/m to 250 N/m.[8] In order to apply AFM-based methods in quantitative assessments of the effects of different microfabrication techniques and surface treatments on fracture properties of nanoscale components, and mechanical properties of MEMS components more broadly, methods are required that are well-suited to the calibration of very stiff cantilevers. Such methods should specify the calibration accuracy (how closely the mean calibrated value estimates the true value) and precision (how closely repeated measurements distribute about the mean value).[9]

In this work, a method is described for calibrating very stiff AFM cantilevers that incorporates specifications of accuracy and precision, and which can be used *in situ* with many different cantilevers for experimental mechanical properties measurements. The method is based on a SI (International

a)Author to whom correspondence should be addressed. Electronic mail: atz2@cornell.edu

System of units)-traceable measurement chain. Certified reference masses are used to calibrate a load cell which is in turn used to calibrate an instrumented indenter. The indenter is then used to calibrate the stiffness of a reference cantilever using methods previously described: stiffness range 1.1 N/m to 11.9 N/m,[10] 0.2 N/m to 250 N/m,[11] and 1.4 N/m to 64 N/m[12] (where greater values reflect measurements performed at points away from the free end of the cantilever). The uncertainty in the stiffness of the reference cantilever sets the lower bound for the accuracy and precision of the method. A test cantilever, with which experimental measurements are to be performed, is then calibrated using the reference cantilever and the selected AFM using methods established previously on compliant cantilevers: stiffness range of reference and test cantilevers of 0.02 N/m to 0.2 M/m,[13] 0.13 N/m to 0.5 N/m,[14] 0.14 N/m to 16.2 N/m,[15] 0.02 N/m to 0.2 N/m,[16] and 1.4 N/m to 3.6 N/m[12] (where the values reflect the response at the end of the cantilever). The measured uncertainty (statistical repeatability) in the stiffness of a test cantilever combined with the traceable uncertainty of the reference cantilever sets the precision of the overall calibration. The procedure has been demonstrated on test cantilevers in the stiffness range 0.02 N/m to 3.6 N/m[12,13] and is here extended to a range around 200 N/m. The difficulty with extending the reference cantilever calibration method into a test cantilever stiffness range of 200 N/m in a traceable way is that the combined reference plus test cantilever displacements (although measured at the mutual ends of the cantilevers, and thus maximized) are very small, leading to decreased precision in AFM optical PSD output. A goal of the present work is to assess the feasibility of extending the reference cantilever method to test cantilevers an order of magnitude stiffer than those examined previously (and into the range covered by the indentation method), while retaining precision and introducing accuracy (traceability). (Recently, National Laboratories have begun to explore the use of commercial and custom mass and force balances as SI-traceable calibration platforms for small force transfer artifacts.[17] These first results focused on *piezoresistive* cantilever artifacts with stiffness values between 1 N/m and 3 N/m, although a stiffer artifact with a stiffness of about 80 N/m was also demonstrated).

Two other methods, a dimensional method using cantilever dimensions and the elastic constants of Si, and another (hybrid dimensional-resonance method) using the cantilever dimensions and resonant frequency along with a finite element model (FEM) of the cantilever, are used to estimate the stiffness of the test cantilever and compared with the reference cantilever calibration. Finally, an example is given of the use of a calibrated test cantilever in the fracture strength testing of Si nanobeams.

II. STIFFNESS CALIBRATION METHODS AND RESULTS

A. Reference cantilever method

The use of a reference cantilever of known stiffness for calibration of the stiffness of a test cantilever for performing AFM measurements of small-scale mechanical properties is a multi-step process: (1) Load cell calibration,[18] (2) Instrumented indenter calibration,[18] (3) Reference Cantilever calibration,[10–12] and (4) Test cantilever calibration.[12–18] The steps used here, along with the introduced uncertainties, are described below in turn.

1. Load cell calibration

A capacitance-based load cell described previously[18] was calibrated using deadweight masses and an Andeen-Hagerling (Cleveland, OH) AH 2500A capacitance bridge.[19] The masses, m, were NIST-certified (traceable back to a realization of a base unit of the SI system, in this case the kilogram) and ranged from nominally 0.5 mg to 500 mg and the applied force, $F = mg$, exerted by a mass on the load cell was calculated using a locally measured SI-traceable value of gravitational acceleration, g. The greatest uncertainty in the applied force was for the smallest mass (exerting nominally 5 μN force) and was $\pm 0.1\%$ (all uncertainties in this paper quoted as percentages are relative uncertainties: the uncertainty in a quantity divided by its mean or best estimated value). Application of a mass to the load cell resulted in a change in cell capacitance, ΔC; once again the greatest uncertainty in the capacitance change was for the smallest mass and was $\pm 0.2\%$ (uncertainty in the capacitance output arose primarily from the resolution of the capacitance bridge). The load cell was calibrated by fitting the force-capacitance change data to a cubic polynomial of the form $F = A_3(\Delta C)^3 + A_2(\Delta C)^2 + A_1(\Delta C)$; the greatest residual deviation between the fitted and measured forces was 0.2%.

2. Instrumented indenter calibration

The load and displacement outputs of an instrumented indenter, Hysitron Triboindenter (Eden Prairie, MN), were calibrated using the calibrated capacitance load cell and an optical interferometer, respectively. A spherical probe was loaded onto the load cell. The indentation force recorded by both the indenter internal measurement system and the external calibrated cell were compared. The proportionality constant relating the forces from these two sources provided the calibration of the indenter force output. Repeated applications of nominal forces of 10 μN and 50 μN in the target testing range gave standard deviations in the calibrated indenter mean force output of 1.5% and 0.7%, respectively; additional, small, uncertainty in the indenter force output arose from time variation in the output. Summing all uncertainties in quadrature, from both the capacitance and indenter force systems, resulted in a total indenter force calibration uncertainty (over the force range used) between 1% and 2%. Linearly, interpolating between these values to a force of 25 μN provided a characteristic indenter force uncertainty of $\pm 1.7\%$. The displacement of the indenter was calibrated using an inferometer system of our own design.[20] The system, based on a 1550 nm fiber-optic laser source, used a Fabry-Perot cavity established between the end of the indenter shaft and the specimen mounting stage to measure the displacement of the shaft over a range of travel of 4 μm with an accuracy well below 1 nm. Displacement as

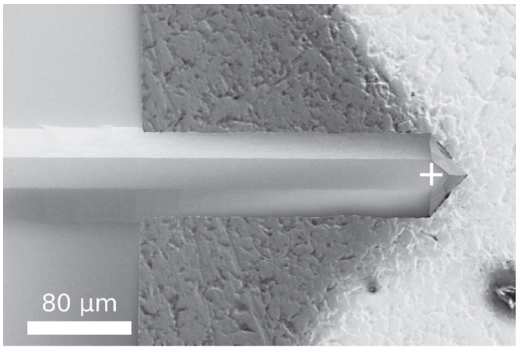

FIG. 1. SEM micrograph of a reference cantilever.

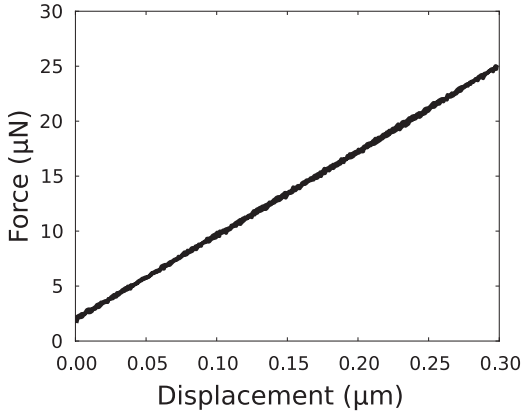

FIG. 2. Single force-displacement response of a reference cantilever.

determined by the inferometer was then compared to the displacement reported by the indenter. Using this method, the uncertainty in the Triboindenter displacement was found to be ±0.3%.

3. Reference cantilever calibration

The stiffness of the reference cantilever, AppNano (Santa Clara, CA), ACL-TL, was calibrated using the calibrated instrumented indenter. The reference cantilever, shown in the scanning electron microscope (SEM) image of Figure 1, was selected for four important characteristics: stiffness, length, tip, and shape. The stiffness was selected to be as close as possible to that of the test cantilevers so as to provide the spring constant matching that reduces uncertainties in the test cantilever calibration process.[14,15] The ACL-TL has a nominal stiffness of 45 N/m, although the group of candidate reference cantilevers was hand selected to have greater than average stiffness of at least 60 N/m. A tipless, picket-shaped, long reference cantilever (Figure 1) was selected to reduce uncertainties in stiffness arising from uncertainty in the loading location of the cantilever. The lack of a tip and the picket end shape enabled repeatable placement of the indentation probe on the reference cantilever using the angular cues of the picket end and without having to avoid a tip. While it would be desirable to have a stiffer reference cantilever to increase spring constant matching, the placement repeatability afforded by the lack of a tip provides a greater reduction in overall uncertainty than the difference in stiffnesses. Repeatability of loading location was within 1 μm; this location is indicated by the white cross superimposed in Figure 1. As the stiffness of a cantilever varies in a cubic manner with distance of the loading location to the clamped, built-in end, long cantilevers reduce stiffness uncertainties arising from uncertainties in the loading location. The reference cantilever was approximately 220 μm long. As the reference cantilever stiffness was calibrated at the exact location used for calibrating the test cantilever there was no need to account for length anomaly corrections.[11,12,16]

A typical reference cantilever force-displacement calibration response obtained using the instrumented indenter is shown in Figure 2, and a schematic diagram of the calibration method is shown in Fig. 3(a). Both loading and unloading data are shown in Fig. 2 and the response displays little noise or hysteresis and excellent linearity. The slope of this line provides the reference cantilever calibrated stiffness and the standard error of the slope provides the stiffness uncertainty for that particular measurement. For the reference cantilever used in this study, the calibration was repeated 20 times (10 times on two different days) providing a calibrated stiffness value, k_{ref}, of 76.7 ± 0.6 N/m, where the uncertainty represents the statistical repeatability uncertainty of one standard deviation. Combining this uncertainty in quadrature with the instrumented indenter calibration uncertainty provides a total reference cantilever stiffness uncertainty of ±1.9%.

4. Test cantilever calibration

The stiffness of the test cantilever, an uncoated TAP525, Bruker AFM Probes (Camarillo, CA), MPP-13100-10 with a nominal stiffness of 200 N/m was calibrated using the previously calibrated reference cantilever and an AFM, Bruker Dimension 3100 (Santa Barbara, CA). Bottom- and side-view SEM images of the test cantilever are shown in Figure 4. The test cantilever calibration was a two-step process. In the first step, the reference cantilever was mounted on a stiff substrate on the AFM stage and the test cantilever was clamped in the piezoelectric scanning system of the AFM in the usual manner. The tip at the free end of the test cantilever was then placed over the bulk Si base of the reference cantilever and the clamped end of the test cantilever displaced in the vertical direction by the AFM piezoelectric drive. Contact of the test cantilever tip with the reference cantilever base led to deflection of the test cantilever and a change in the PSD output signal. If the reference cantilever base is approximated as rigid, the displacement of the free end of the test cantilever relative to the clamped end is equal to the imposed AFM piezoelectric displacement; the ratio of the imposed displacement to the PSD output voltage is then the optical lever sensitivity of the AFM, S_1. A representative plot of output voltage as a function of imposed piezoelectric displacement enabling the determination of S_1 is shown in Figure 5: Initially, the PSD output voltage was invariant as the cantilever approached the base surface. As the tip approached the surface, the output decreased slightly reflecting van der Waals interactions between the tip and the surface and a small attractive tip-surface

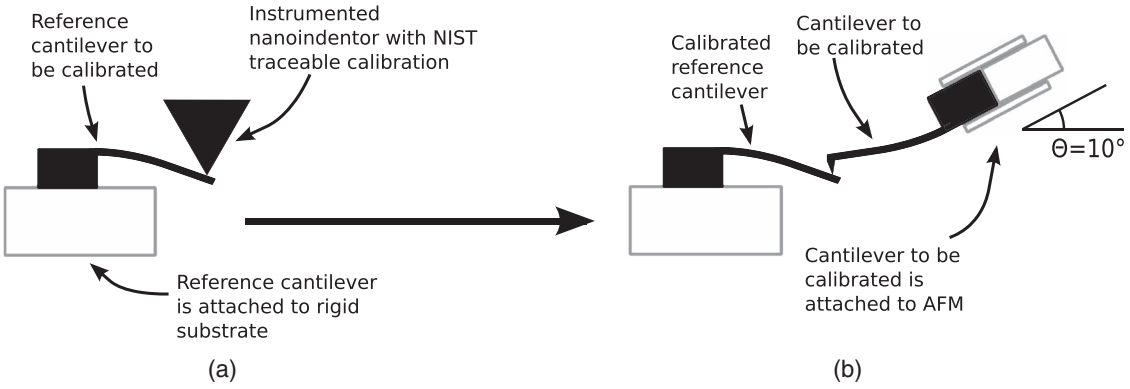

FIG. 3. Schematic diagram of a reference cantilever deformed by indenter (a) and then test cantilever (b).

interaction. Once the tip was fully in contact with the surface the PSD output increased linearly as the cantilever deflected upward in a repulsive interaction. The inverse slope of this linear variation is S_1.

In the second step, the tip of the test cantilever was aligned over the free, picket-end, location at which the reference cantilever was calibrated and a second PSD output-imposed displacement response was measured. The test cantilever pushed on the reference cantilever and both deflected, as shown in Fig. 3(b), acting as springs in series. Hence, the AFM head traveled through a greater distance to produce the same test cantilever deflection. As a consequence, the slope of the resulting linear region of the response in the second step was less than that in the first, as shown in Figure 5. The inverse of this second slope is S_2. The stiffness of the test cantilever, k, can be determined from S_2, S_1, and k_{ref}, after correcting for the orientation of the test cantilever. The test cantilever was mounted in the AFM head at an angle, θ, of 10° relative to the reference cantilever, as shown in Figure 3(b). The stiffness of the test cantilever is given by[16]

$$k = \left(\frac{S_2}{S_1} - 1\right) k_{\text{ref}} \cos^2(\theta). \quad (1)$$

Ten measurements of the test cantilever response to determine S_1 and S_2 were taken over two days (five each day) which generated a repeatability uncertainty for k of 7.2%. The mean values for S_1 and S_2 were 63.14 nm/V and 270.7 nm/V, respectively. The test cantilever was remounted and laser spot adjusted before each measurement to make each measurement as independent as possible. Combining this value with the reference cantilever stiffness uncertainty (1.9%) led to a total uncertainty of the test cantilever stiffness of ±7.4%, or, using the mean values of S_1 and S_2, $k = 218 \pm 16$ N/m.

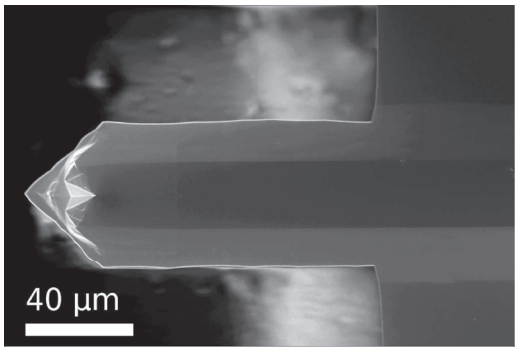

(a)

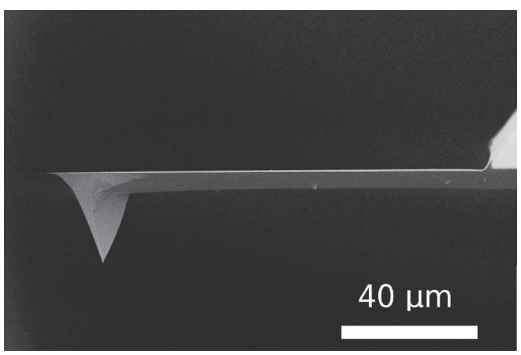

(b)

FIG. 4. Top and side view SEM micrographs of a test cantilever.

B. Dimensional method

The stiffness of the test cantilever can be estimated based on the cantilever dimensions, geometry, and the elastic properties of Si. Figure 6 shows a schematic diagram of the test cantilever. The length dimension L, the short and long lateral dimensions a and b, and the thickness t may all be measured using SEM or some other method. The finite element method

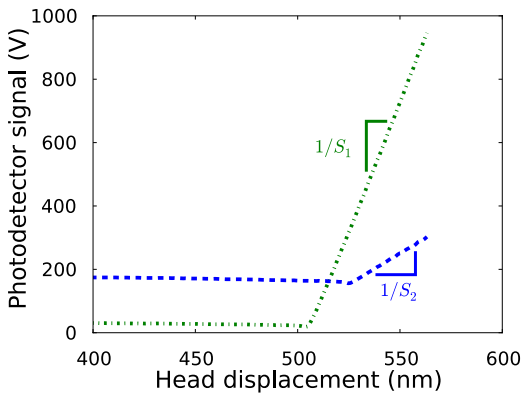

FIG. 5. S_1 and S_2 measurement data with linear fits.

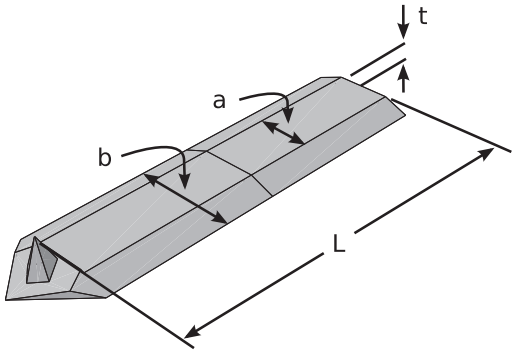

FIG. 6. Schematic diagram of test cantilever, showing dimensions.

is used for the stiffness computation and an analytical approximation is used as the basis for the uncertainty analysis.

To analyze the uncertainty, a beam theory based analytical approximation for the stiffness of the cantilever is used:

$$k = \frac{E_{\{110\}[110]} t^3 \left(a^2 + 4ab + b^2\right)}{12L^3 (a+b)}, \tag{2}$$

where $E_{\{110\}[110]}$ is the Young's modulus of Si in the [110] direction (along the axial direction of the cantilever) with parallel {110} plane (in this case the top or bottom surface of the cantilever) in a state of plane strain perpendicular to the (001) a and b faces and is given by[21]

$$E_{\{110\}[110]} = C_{44} + \frac{(C_{11} + 2C_{12}) \cdot (C_{11} - C_{12})}{2C_{11}} \tag{3}$$

with C_{11} = 165.77 GPa, C_{12} = 63.924 GPa, and C_{44} = 79.619 GPa.[22] The orientation of the cantilever was confirmed using Laué X-ray back reflection. The SEM measured values for L, a, b, and t were 112 μm, 24.7 μm, 54.6 μm, and 6.12 μm with repeatabilities of 0.81%, 2.4%, 0.74%, and 4.6%.

The relative uncertainty in k using this method can be calculated by applying propagation of variance[23] to Eq. (2) resulting in

$$\begin{aligned}\left(\frac{\delta k}{k}\right)^2 = &\left(3\frac{\delta t}{t}\right)^2 + \left(3\frac{\delta L}{L}\right)^2 \\ &+ \left(\frac{a^3 + 2a^2b + 3ab^2}{a^3 + 5a^2b + 5ab^2 + b^3}\right)^2 \left(\frac{\delta a}{a}\right)^2 \\ &+ \left(\frac{3a^2b + 2ab^2 + b^3}{a^3 + 5a^2b + 5ab^2 + b^3}\right)^2 \left(\frac{\delta b}{b}\right)^2 \\ &+ \left(\frac{\delta E_{\{110\}[110]}}{E_{\{110\}[110]}}\right)^2. \end{aligned} \tag{4}$$

Substituting in the measured values and repeatabilities for L, a, b, t, and $E_{\{110\}[110]}$, using McSkimin's values for uncertainty in elastic moduli of Si,[22] the maximum uncertainty is estimated to be 13.9%. This value is almost entirely controlled by uncertainty in t, which when multiplied by its weighting factor of 3 contributes 13.6% to the 13.9% total uncertainty in k.

Stiffness is computed using finite element analysis which allows incorporation of effects such as the asymmetry of the cantilever base (see Figure 4). The FEM model used the measured cantilever dimensions and elastic moduli and gave a stiffness of k = 231 N/m. Taking into account the uncertainty analysis results in a stiffness of $k = 231 \pm 32$ N/m.

C. Hybrid dimensional-resonance method

In experiments where stiff cantilevers were used to measure the fracture strength of Si nanobeams,[6,7] cantilever stiffness was measured using a hybrid dimensional-resonant frequency method. In this case, only a top view SEM image, such as Figure 4(a) was available. While the L, a, and b may be measured using Figure 4(a), the thickness dimension t is left unknown. In addition to measuring L, a, and b, the resonant frequency ω_0 was also measured in this method. The thickness of a finite element model was tuned so that the resonant frequency of the model matched the measured frequency. Once the frequencies were matched, the stiffness was calculated using the finite element model. Using this method results in a stiffness of k = 183 N/m.

The uncertainty in this method depends on uncertainty in the measured dimension L, a, and b as well as the uncertainty in Young's modulus $E_{\{110\}[110]}$ and resonant frequency. The relative uncertainty in density of Si is 1.1×10^{-7} and considered negligible in this analysis.[24] A final source of error is the mass of the cantilever tip, m_{tip}. Because only a top view SEM image is used for dimensional measurements the length of the tip cannot be determined and the manufacturer nominal values must be used. This results in a large uncertainty in m_{tip} of 44.8%. Treating the tip as a point mass at the end of the cantilever, resonant frequency may be expressed as

$$\omega_0^2 = \frac{k}{m_{\text{tip}} + CM}, \tag{5}$$

where M is the mass of the body of the cantilever and C = 0.23 is a scaling factor allowing the distributed mass of the cantilever to be expressed as a point oscillator.[25] M may be expressed in terms of cantilever dimensions and the density of Si, ρ,

$$M = \rho L t (a+b)/2. \tag{6}$$

Combining Eqs. (5) and (6) with Eq. (2) relates cantilever thickness to measured parameters,

$$\omega_0^2 = \frac{E t^3 \left(a^2 + 4ab + b^2\right)}{12L^3 (a+b)} \frac{1}{m_{\text{tip}} + 1/2C\rho L t (a+b)}. \tag{7}$$

A computer algebra system was used to exactly solve Eq. (7) for t, giving t as a function of measured parameters, $t = t(E_{\{110\}[110]}, a, b, L, m_{\text{tip}}, \omega_0)$. Uncertainty in t can then be found using propagation of variance analysis[23] (due to their complexity, the explicit forms of the partial derivatives are

omitted here),

$$\left(\frac{\delta t}{t}\right)^2 = \left(\frac{E_{\{110\}[110]}}{t}\frac{\partial t}{\partial E_{\{110\}[110]}}\frac{\delta E_{\{110\}[110]}}{E_{\{110\}[110]}}\right)^2 + \left(\frac{a}{t}\frac{\partial t}{\partial a}\frac{\delta a}{a}\right)^2 + \left(\frac{b}{t}\frac{\partial t}{\partial b}\frac{\delta b}{b}\right)^2 + \left(\frac{L}{t}\frac{\partial t}{\partial L}\frac{\delta L}{L}\right)^2 + \left(\frac{m_{\text{tip}}}{t}\frac{\partial t}{\partial m_{\text{tip}}}\frac{\delta m_{\text{tip}}}{m_{\text{tip}}}\right)^2 + \left(\frac{\omega_0}{t}\frac{\partial t}{\partial \omega_0}\frac{\delta \omega_0}{\omega_0}\right)^2 = \left(-0.333\frac{\delta E_{\{110\}[110]}}{E_{\{110\}[110]}}\right)^2 + \left(-0.142\frac{\delta a}{a}\right)^2 + \left(-0.192\frac{\delta b}{b}\right)^2 + \left(1.000\frac{\delta L}{L}\right)^2 + \left(0.333\frac{\delta m_{\text{tip}}}{m_{\text{tip}}}\right)^2 + \left(0.667\frac{\delta \omega_0}{\omega_0}\right)^2 = 14.9\%. \quad (8)$$

In this case, uncertainty is dominated by m_{tip}. All other terms contribute less than 1% uncertainty when multiplied by their weighting factor. Using Eq. (2), uncertainty in stiffness is $\delta k/k = 3\delta t/t = 45\%$ or a stiffness value of $k = 183 \pm 82$ N/m.

D. Summary of stiffness calibration results

The stiffness values and uncertainties of each method are summarized in Table I. Note that in addition to being SI-traceable, the reference cantilever method has the smallest uncertainty of the three methods. Thus, the reference cantilever method is of great benefit in experiments such as the AFM based stochastic fracture testing of nanostructures, discussed below, where accurate stiffness calibration is required to quantitatively measure strength and small uncertainty is needed to discern actual strength variations.

III. EXAMPLE APPLICATION: STRENGTH TESTING

As mentioned in the Introduction, stiff AFM cantilevers are extremely useful for applying the large forces required to test mechanical properties of micro- and nano-scale devices. In this section, an example application of the use of a stiff AFM cantilever, the calibrated test cantilever described in Sec. II, is given in the brittle-fracture strength testing of Si nanobeams. The example highlights the importance of both accuracy and precision in calibration of the cantilever stiffness in enabling valid strength measurements.

The rapid development of MEMS and nanoelectromechanical systems (NEMS) necessitates the ability to predict and control the strength of micro-and nano-scale structures. In a recent survey of the strength of single crystal Si[26] (a material widely used in MEMS and NEMS), the strong dependence of Si strength on both component fabrication method and size was highlighted. The survey made clear that surface flaws introduced by the fabrication process were the dominant factor in controlling the strength of Si components and that flaws were larger (and hence strengths smaller) in larger components. For nano-scale components, the strengths approached the ideal value (about $E/10$, which for Si is about 16 GPa): Si nanowires (diameters < 100 nm) with as-grown, near-pristine, surfaces, exhibit strengths that depend on wire diameter and that are comparable to the ideal value.[27] Fabricated nano-scale Si beam structures (dimensions approximately 100 nm) also have strengths approaching the ideal value and that are strongly dependent on both the surface roughness and surface oxidation.[6,7] Such Si nanobeams are the focus of this example.

TABLE I. Summary of stiffness values and uncertainties for the three methods discussed.

Method	Stiffness (N/m)	Uncertainty
Reference cantilever	218 ± 16	7.4%
Dimensional	231 ± 32	13.9%
Hybrid dimensional-resonance	183 ± 82	45%

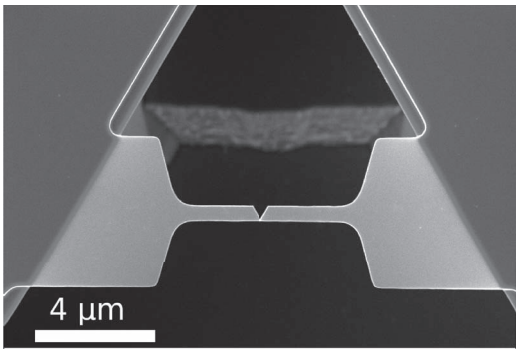

FIG. 7. SEM micrograph of a Si nanobeam after fracture testing.

The Si nanobeams were fabricated and tested as described earlier.[6,7] Briefly, the beams were fabricated from {111} oriented Si wafers and were approximately 12 μm long, 500 nm wide, and 100 nm thick. The beams were doubly clamped and under-etched so that they were freely suspended across a trench. An example is shown in Figure 7. The calibrated AFM test cantilever was used to deform the beam structures until failure, as shown in Figure 8. The test cantilever was brought into contact with a nanobeam and the applied AFM piezoelectric displacement, δ_{piezo}, increased until the nanobeam failed. The displacement of the test cantilever, $\delta_{\text{cantilever}}$, was determined from the calibrated AFM PSD output voltage. The displacement of the nanobeam throughout the test was given by $\delta_{\text{beam}} = \delta_{\text{piezo}} - \delta_{\text{cantilever}}$ and the

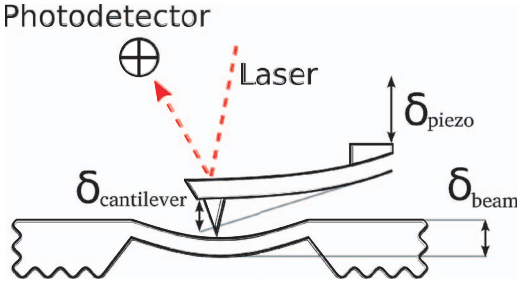

FIG. 8. Schematic diagram of nanobeam loading.

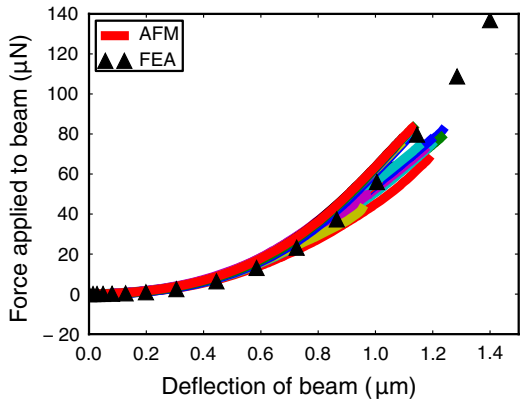

FIG. 9. Force-displacement responses of nanobeams and FEM predictions.

force applied to the nanobeam by the cantilever was given by $F_{\text{beam}} = k\delta_{\text{cantilever}}$.

Figure 9 shows the force-displacement behavior measured for 23 nominally identical Si nanobeams. Each solid line corresponds to an individual beam and failure is indicated by termination of a line. The force-displacement behavior is nonlinear due to the large displacements required to fracture the beams relative to the beam thickness. The black triangles in Figure 9 correspond to forces and displacements calculated using a FEM prediction for the beams.[6] The agreement between the FEM prediction and the measured force-displacement responses is a reflection of the accuracy of the test cantilever stiffness calibration. That is, the calibration generated the correct value of the stiffness in agreement with other, independently specified, quantities, in this case the elastic constants of Si and the nanobeam dimensions. For clarity, the 7.4% uncertainty in the forces is not shown in Figure 9, but corresponds to about 6 μN for the greatest failure force observed.

The finite element model used to calculate the data depicted in Figure 9 can also be used to calculate maximum stress at failure, shown in Figure 10, in this case ranging from about 12 GPa to 20 GPa. This range of strengths aligns well with what was observed in past experiments.[6,7] The solid line is a Weibull fit with scale parameter 17.5 GPa and shape parameter 7.75. The error bars shown in Figure 10 only show the

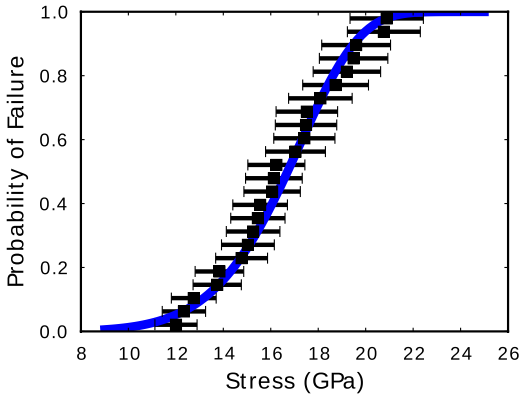

FIG. 10. Cumulative failure probability vs strength for Si nanobeams with Weibull fit.

7.4% uncertainty due to cantilever stiffness. In reality other sources of error exist as well, such as uncertainty due to sampling a random strength distribution with a finite number of points.

IV. CONCLUSIONS

The reference cantilever method provides a traceable path for test cantilever stiffness calibration, and therefore accuracy. As the cantilever is deflected in a similar way during calibration and testing, the calibration is as direct as possible, and hence provides the least limitation on precision. Once calibrated, a reference cantilever can be used to calibrate many test cantilevers, or other MEMS- or NEMS-scale components or devices. Drawbacks include the effort required to calibrate a reference cantilever and that the tip of the test cantilever contacts a surface prior to testing (although this must be done in any event to obtain the AFM optical lever sensitivity). Accurate and precise calibration of stiffness of the stiff cantilevers required for AFM-based measurement of mechanical properties of MEMS- and NEMS-scale devices enable direct comparison of absolute values of quantities obtained with other measurements or models and enable increased certainty in establishing processing-structure-properties relations for materials at the nanoscale.

ACKNOWLEDGMENTS

This work was funded by the National Science Foundation (NSF) Grant No. CMMI-0856488 and the NSF IGERT graduate traineeship in Nanoscale Control of Surfaces and Interfaces (NSF Grant No. DGE-0654193). It was performed in part at the Cornell NanoScale Facility, a member of the National Nanotechnology Infrastructure Network, which is supported by NSF Grant No. ECS-0335765, and made use of the X-ray diffraction facility of the Cornell Center for Materials Research (CCMR) with support from the National Science Foundation Materials Research Science and Engineering Centers (MRSEC) program (DMR-1120296). The usage of the nanoindenter was completed at the National Institute of Standards and Technology in Gaithersburg, MD.

[1]C. Stroh, H. Wang, R. Bash, B. Ashcroft, J. Nelson, H. Gruber, D. Lohr, S. M. Lindsay, and P. Hinterdorfer, Proc. Natl. Acad. Sci. U.S.A. **101**, 12503 (2004).
[2]Y. F. Dufrene, J. Bacteriol. **184**, 5205 (2002).
[3]B. Bhushan and V. N. Koinkar, Appl. Phys. Lett. **64**, 1653 (1994).
[4]*NanoScope V Controller Manual*, Veeco Instruments, Inc., 2006.
[5]B. Ohler, "Practical advice on the determination of cantilever spring constants," Technical Report, Veeco Instruments, Inc., 2007.
[6]T. Alan, M. A. Hines, and A. T. Zehnder, Appl. Phys. Lett. **89**, 091901 (2006).
[7]T. Alan, A. T. Zehnder, D. Sengupta, and M. A. Hines, Appl. Phys. Lett. **89**, 231905 (2006).
[8]T. Alan, "Improving fracture properties of MEMS components by surface control," Ph.D. thesis (Cornell University, 2007).
[9]B. N. Taylor and C. E. Kuyatt, "Guidelines for evaluating and expressing the uncertainty of NIST measurement results," Technical Report 1297, NIST (1994).
[10]J. D. Holbery, V. L. Eden, M. Sarikaya, and R. M. Fisher, Rev. Sci. Instrum. **71**, 3769 (2000).
[11]Z. C. Ying, M. G. Reitsma, and R. S. Gates, Rev. Sci. Instrum. **78**, 063708 (2007).

[12]C. A. Clifford and M. P. Seah, Meas. Sci. Technol. **20**, 125501 (2009).
[13]A. Torii, M. Sasaki, K. Hane, and S. Okuma, Meas. Sci. Technol. **7**, 179 (1996).
[14]C. T. Gibson, G. S. Watson, and S. Myhra, Nanotechnology **7**, 259 (1996).
[15]M. Tortonese and M. Kirk, Proc. SPIE **3009**, 53–60 (1997).
[16]R. S. Gates and M. G. Reitsma, Rev. Sci. Instrum. **78**, 086101 (2007).
[17]M. S. Kim, J. R. Pratt, U. Brand, and C. W. Jones, Metrologia **49**, 70 (2012).
[18]J. R. Pratt, J. A. Kramer, D. B. Newell, and D. T. Smith, Meas. Sci. Technol. **16**, 2129 (2005).
[19]Certain commercial equipment, instruments, or materials are identified in this paper to adequately specify the experimental procedure. Such identification does not imply recommendation or endorsement by the National Institute of Standards and Technology, nor does it imply that the materials or equipment identified are necessarily the best available for the purpose.
[20]D. T. Smith, J. R. Pratt, and L. P. Howard, Rev. Sci. Instrum. **80**, 035105 (2009).
[21]R. S. Gates and J. R. Pratt, Meas. Sci. Technol. **17**, 2852 (2006).
[22]H. J. McSkimin and P. Andreatch, J. Appl. Phys. **35**, 2161 (1964).
[23]H. H. Ku, J. Res. Natl. Bur. Stand. **70C**, 263 (1966).
[24]K. Fujii, M. Tanaka, Y. Nezu, A. Sakuma, A. Leistner, and W. Giardini, IEEE Trans. Instrum. Meas. **44**, 542 (1995).
[25]A. G. Piersol and T. L. Paez, *Harris' Shock and Vibration Handbook*, 6th ed. (McGraw-Hill, 2010).
[26]M. S. Gaither, F. W. DelRio, R. S. Gates, and R. F. Cook, J. Mater. Res. **26**, 2575 (2011).
[27]G. Stan, S. Krylyuk, A. V. Davydov, and R. F. Cook, J. Mater. Res. **27**, 562 (2012).